Morgan & Childs 2/2/2015 9:49 AM
Prepared for submission to Physical Review E

# Study of striations in a spherically symmetric Hydrogen discharge

W. Lowell Morgan[1] and Montgomery W. Childs[2]

[1]*Kinema Research & Software, LLC, P. O. Box 1147, Monument, CO 80132 USA*

[2]*Aurtas International, Inc., 7 Highland Drive, Horseshoe Highlands, Oro Medonte Ontario, L0L-2L0 Canada*

**Abstract**

Experiments on a high power spherically symmetric positive corona discharge in molecular hydrogen are reported upon. These are collisional plasmas in the $H_2$ pressure range of about 0.75 Torr to 3 Torr. Applied voltages ranged up to 600 V on the anode with currents ranging up to 3 A. As in prior published experiments going back to 1997 we observed spherically symmetric striations or double layers. Others have observed such striations in $O_2$, $CO_2$, and mixtures of $N_2$ and acetone or methanol, or benzene. Like $H_2$ all these gases, except $N_2$ itself, readily dissociate and form negative ions by dissociative attachment with electrons. We propose that the striations are instabilities arising from copious formation of negative ions that modify the radial space charge and electric field distributions in such high aspect ratio spherical discharges.

## I. BACKGROUND

In 1997 Nerushev, et al.[1, 2] published their observations of spherical striations or double layers in an anode centered spherically symmetric discharge. Although striations are well known phenomena, having been observed in linear discharges since the mid-19$^{th}$ century, the observations by Nerushev, et al. are among the first in a spherical discharge. There have been a number of publications since 1998 exploring various aspects of the stratification phenomena [3-7].

The publications presenting numerical data from measurements are:

(1) Novopashin, et al.[3] observed concentric spherical striations in a 1:1 mixture of $N_2$ and acetone ($(CH_3)_2CO$), i.e. vapor at a partial pressure of 100 mTorr. They used a simple probe to measure the radial potential distribution $\phi(r)$ finding that, although it decreases monotonically with increasing radius, it possesses local minima, i.e. potential wells, and maxima corresponding to the double layers. The electric field, $E = -\partial\phi(r)/\partial r$ then oscillates correspondingly above and below $E = 0$. $E < 0$ has the field directed toward the anode and for $E > 0$ the field vector is pointed radially outward.

(2) Novopashin, et al.[4] in the same mixture of $N_2$ and acetone used a Langmuir probe to measure the absolute electron temperature $T_e(r)$ and the relative electron density $N_e(r)$ across the striated plasma. They found that $T_e(r)$

declined from ~ 8 eV to ~ 4 eV to a double layer and then jumped over a very small $\Delta r$ and then declined again to the next double layer to ~ 4 eV, and so on. $N_e(r)$ slowly declined over a striation, then dropped precipitously at a double layer, and then slowly declined again, to the next striation boundary, and so on in a stair step fashion.

(3) Belikov and Sakhapov [7] performed their experiments in $N_2$ and acetone mixtures as well as in methanol ($CH_3OH$). Using a mass spectrometer they correlated the times that the striations turned on and off with the dissociation of the $CH_3OH$. The primary dissociation products were CO and $H_2$ with secondary products being $CH_4$, $CO_2$, and OH.

## II. OUR EXPERIMENT

The experiment that we are describing here consists of a large bell jar that can be pumped down to a gas pressure of about ten microns. The anode is a ¼" (~0.6 cm) diameter iron sphere powered by a variable DC power supply capable of providing 3 Amp at 600 Volts. We have a variety of shapes and sizes of cathodes, all copper, that we work with. They all have a stand-off distance from the anode of many anode radii.

The topology of the grounded cathode has only a perturbative effect upon the plasma for the following reason. If we consider a pair of concentric spheres with the smaller inner sphere of radius $R_i$ being the powered electrode and the larger outer sphere of radius $R_o$ being grounded, the radial electrostatic field between spheres is

$$E(r) = V_o R_i R_o/(R_o - R_i)r^2$$

where $V_o$ is the potential of the inner electrode relative to the ground. If the radius of the outer electrode is much greater than that of the center electrode, i.e. $R_o >> R_i$, then

$$E(r) \simeq V_o R_i/r^2$$

Thus the size and shape of the outer electrode are largely irrelevant. It acts as only a perturbative influence upon the electric field near the powered electrode, which is the anode in our device.

Due to the large separation between anode and ground this is a positive corona discharge. A high voltage $V_o$ creates a large enough electric field that gas breakdown occurs out to a short distance from the anode. The electrons and negative ions produced drift toward the anode and the positive ions drift and diffuse out into the surrounding gas. The creation of space charge in the plasma modifies the electric potential $\phi(r)$ and, consequently, E(r) substantially.

## III. EXPERIMENTAL OBSERVATIONS: STRIATIONS

We ran the electric discharge in hydrogen at gas pressures ranging from about 50 mTorr to 10 Torr. We are interested in various anode phenomena and in the striation phenomena. We did not have access to a Langmuir probe but did use a mass spectrometer and state of the art digital spectrometer.

Multiple concentric plasma spheres or striations were readily observed over the pressure range from a half Torr to about 3 Torr. Figure 1 shows a photograph of such a striated plasma.

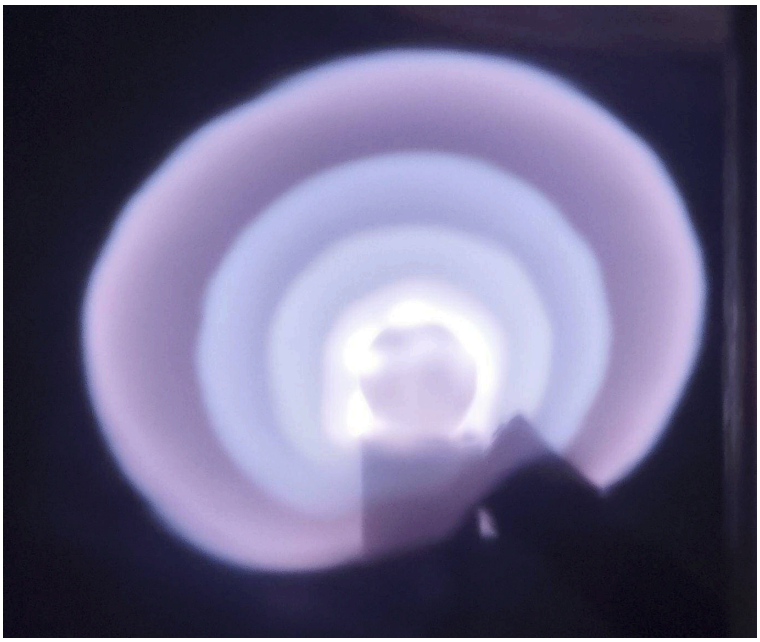

**Figure 1 Double layers surrounding anode.**

Performing a density scan of the image from the center of the anode outward produced the following graph of light intensity as a function of E radius:

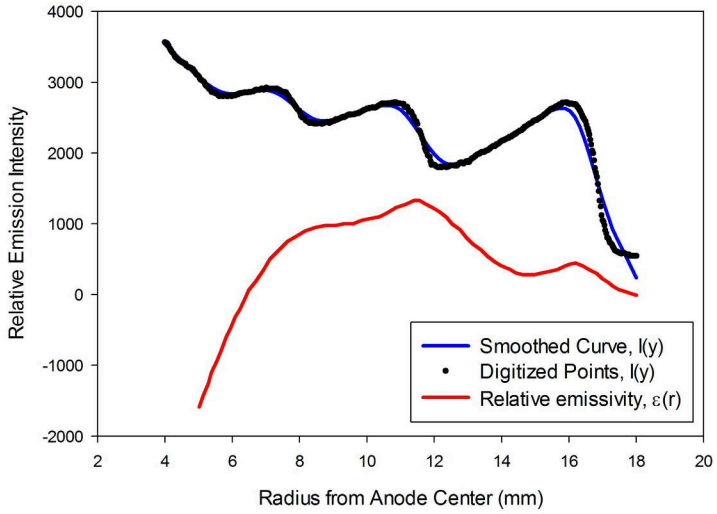


**Figure 2 Measured relative radial light intensity and relative emissivity computed from Abel transform.**

Note that due to the approximately logarithmic response of the CCD to light intensity this is more like the logarithm of the intensity. The edges of the zones correspond to "dark spaces", because, as we will see, the E-field vector goes through zero so that there is very little excitation in those regions. Nerushev, et al. [2] observed that spacing of the striations follows a power law or exponential function. That is true of these as well.

The light intensity as a function of r cannot be observed directly because the line of sight is along a chord passing through the multiple shells each point of which is at a different radius from the anode. For an optically thin plasma Abel's transform can be used to obtain the emissivity $\varepsilon(r, \lambda)$ where r is the radius from the anode, from the observed light intensity $I(y, \lambda)$, where the y-axis is along the radius from the anode perpendicular to the line of sight. Abel's transform is based only upon geometrical considerations. The emissivity $\varepsilon(r, \lambda)$ is related to $I(y, \lambda)$ by

$$\varepsilon(r, \lambda) = -(1/\pi) \int_r^R \left[ dI\ (y,l) / \ dy \right] / \ \left( y^2 - r^2 \right)^{1/2} dy$$

where R is the outer radius of the sphere of observation. The calculated $\varepsilon(r)$ is also shown in Fig. 2. Note that, although it oscillates, it has a well defined peak value about three anode radii from the anode surface.

In an optically thin plasma we have coronal equilibrium such that states having a large A-coefficient are in a steady state where

$$dN^*/dt = k_{ex} N_e N - A N^*$$

or, at steady state,

$$N^* = k_{ex} N_e N/A$$

$N^*$ is the density of the excited state, N the density of the ground state, $N_e$ the electron density, and $k_{ex}$ the electron impact excitation rate coefficient.

So the emissivity $\varepsilon(r, \lambda)$ is

$$\varepsilon(r, \lambda) = (h\nu)\, A\, N^*(r) = (h\nu)\, k_{ex}(r)\, N_e(r)\, N \quad (\text{Watts/cm}^3)$$

This gives us a "direct" measure of $k_{ex}(r)\, N_e(r)$, which we will discuss in detail later on. $\varepsilon(r, \lambda)$ is relative, so we can choose an $r_o$ and calculate the ratio

$$\varepsilon(r)/\varepsilon(r_o) = k_{ex}(r)\, N_e(r)/k_{ex}(r_o)\, N_e(r_o)$$

The excitation rate coefficient is a function of the local electric field or, in terms of the similarity parameter in Boltzmann's equation that describes the electron kinetics in a collisional plasma, E/N or E/p where N is the gas density $\text{cm}^{-3}$ and p is the neutral gas pressure (Torr), so, $k_{ex}(r)$ is more correctly $k_{ex}[E/N(r)]$ or $k_{ex}[E/p(r)]$.

The excitation rate coefficient is just the average

$$k_{ex}[E/N(r)] = \langle v_e[E/N(r)]\, \sigma_{ex}(v_e) \rangle$$

where $v_e$ is the random "thermal" speed of an electron and $\sigma_{ex}$ is the electron impact excitation cross section for the radiating atomic or molecular state. We have enclosed the word thermal in quotation marks because very generally the speed distribution of the electrons is non-thermal or non-Maxwellian. This will be discussed further below. The excitation cross sections $\sigma_{ex}$ are well established for a large number of atoms and molecules.

## IV. CORONA DISCHARGE PHYSICS AND THE PLASMA CHEMISTRY OF $H_2$ AND H

### A. The positive corona

In the most simple description of a positive corona discharge the plasma volume consists of an ionization region where E/N(r) is large enough to ionize the atoms and molecules in the gas and a unipolar region comprising various species of positive ion drifting and diffusing toward the cathode ground. This unipolar region has been discussed and described analytically in great detail by Sigmond [8] and many other authors. This work is not concerned with the unipolar region.

In the ionizing region the E-field or E/N(r) is large enough for net electron gain due to electron impact ionization of $H_2$, H, and whatever other species, iron vapor from the anode for example, may be present in the gas. In some regions of the plasma

ionization of electronically excited states may contribute significantly to the plasma density as may photo-ionization.

This ionization may be balanced in steady state by a combination of dissociative recombination of electrons with the $H_2^+$ and $H_3^+$ positive ions and transport of electrons and ions out the ionization region by field driven drift and by diffusion. Typically $H_3^+$ is the most abundant molecular ion. We found that to be the case in our mass spectra. There can also be some stabilization of the discharge due to dissociative attachment of $H_2$, i.e. $e + H_2 \rightarrow H + H^-$, but, as we discuss below, negative ion formation can also lead to instabilities. Unlike most low pressure linear discharges in a tube in which the walls of the tube play a significant role in plasma stability, this spherical corona is a volume dominated plasma.

### B. Hydrogen plasma chemistry and the double layers

Figure 3a shows the details of the first potential well taken from the published probe measurements of Novopashin, et al.[3].

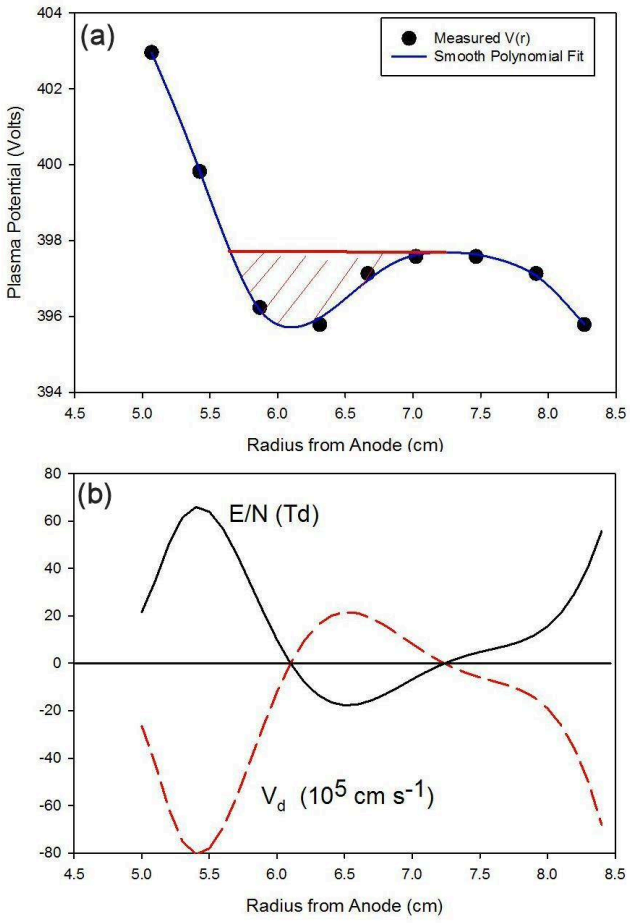


**Figure 3 Upper curve (a): measured well in plasma potential; Lower curves (b): corresponding E(r)/N and calculated drift velocity assuming constant N(r).**

Using the smoothed curve through their measured points we have calculated and graphed in Fig. 3b the values of E/N(r) and $V_d$[E/N (r)] in that region. $V_d$ is the electron drift velocity to which the electron current density is related by $j(r) \equiv -eN_e(r)V_d(r)$. The electron current flows, on average, inward toward the anode. These are estimates because we do not know the true N(r) due to the effects of gas heating and molecular dissociation.

The striations have been observed to occur in $O_2$ and $CO_2$ as well as acetone, methanol, and benzene plasmas but not in $N_2$, He, or Ar. Something that $H_2$ as well as $O_2$, $CO_2$, acetone, methanol, and benzene have in common is that they readily dissociate due to electron impact and they readily form for negative ions by dissociative attachment. The importance of this will become apparent below.

The plasma chemistry of $H_2$ is understood in detail. We are beneficiaries of the work on hydrogen of the late A.V. Phelps and his collaborators over 50 years from Ref. [9] to Ref. [10] and that of M. Capitelli and his collaborators over the past 35 years, which have given us very much collisional and radiative data that are of relevance to hydrogen plasmas. Sophisticated models of hydrogen discharge plasmas have been created over the years using these data [10-13].

We will use here a very simplified model of hydrogen plasma chemistry to illustrate some points. For our purpose we simplify the chemistry to the following reactions:

(1) $H_2 + e^- \rightarrow 2H + e^-$
(2) $H_2 + e^- \rightarrow H_2^+ + 2e^-$
(3) $H_2(v=0) + e^- \rightarrow H_2(v=1) + e^-$
(4) $H_2(v) + e^- \rightarrow H_2(v+1) + e^-$
(5) $H_2(v) + e^- \rightarrow H + H^-$
(6) $H_2^+ + e^- \rightarrow 2H$
(7) $H^- + H \rightarrow H_2 + e^-$
(8) $H^- + H_2^+ \rightarrow H_2 + H$

The electron collision cross sections for processes (1) – (5) are well known. We have used a very complete set of electron-$H_2$ and H collision cross sections [14-16] in our code [17] for solving Boltzmann's equation for the energy distribution of electrons $f_o(\varepsilon)$ in a weakly ionized gas. The most important parameters are, of course, the similarity parameter E/N and the gas density N ($cm^{-3}$). E/N has units of V-$cm^2$ although the units commonly used are Townsends (Td) where 1 Td = $10^{-17}$ V-$cm^2$.

Although $H_3^+$ is likely the dominant positive ion due to the reaction $H_2^+ + H_2 \rightarrow H_3^+ + H$, we have called all the positive ions $H_2^+$ because the dissociative recombination coefficients of the two ions are about the same [18]. The rate coefficients for the important reactions (7) and (8) are well known and can be found in Ref. [19].

Dissociative attachment of electrons to the ground vibrational state of $H_2$, i.e. $H_2(v=0)$ has a very small cross section of $1.6\times10^{-21}cm^2$ at an electron energy of 3.7 eV. On the other hand, the dissociative attachment cross sections increase greatly with $H_2$ vibrational quantum number. For $H_2(v=9)$ the cross section is $4.8\times10^{-16}cm^2$ at 0.13 eV. In a hydrogen plasma we expect there to be a high degree of vibrational excitation.

Figure 4 shows the attachment coefficient $\eta(v)/N \equiv k_{da}(E/N)V_d(E/N)$ for $H_2(v=0)$ to $H_2(v=9)$ as functions of E/N. Also shown as the shaded area is the range of ionization coefficient $\alpha/N \equiv k_iV_d$ between that for pure $H_2$ and that for pure H.

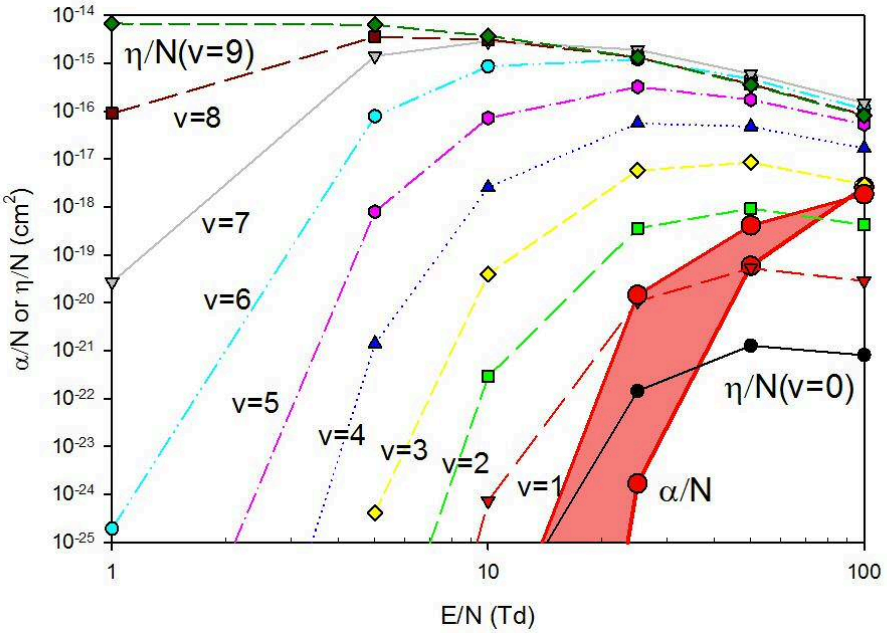


**Figure 4 Computed ionization and attachment coefficients.**

It is clear in Fig. 4 that $\eta(v)/N$ increases by many orders of magnitude as the vibrational quantum number increases. If these vibrational states become highly populated the total rate of $H^-$ negative ion formation will increase accordingly.

The cross section for vibrational excitation $H_2(v=0\rightarrow1)$ by electron impact is $0.5\times10^{-16}cm^2$ at 3.3 eV, which is substantial, but is an order of magnitude greater than that for $H_2(v=0\rightarrow2)$ and two orders of magnitude greater than that for $H_2(v=0\rightarrow3)$. On the other hand the cross sections for $H_2(v\rightarrow v+1)$ are typically about the same as that for $H_2(v=0\rightarrow1)$ [20] so that the vibrational levels of $H_2$ in a plasma can be populated by electron collisions in a ladder-like fashion by a series of $\Delta v=1$ transitions. At higher values of E/N than we are dealing with here the $H_2$ vibrational states can also be populated with 7% to 19% efficiency from excitation and subsequent decay of the $H_2(B^1\Sigma)$ and $H_2(C^1\Pi)$ electronic states [15].

In addition to the electron impact excitation, especially at smaller values of E/N, Vibration-to-Vibration and Vibration-to-Translation energy transfer processes can be significant. The rate coefficients for the $H_2(v) + H_2(v=1) \rightarrow H_2(v+1) + H_2(v=0)$ V-V process and the $H_2(v) + H_2(v=0) \rightarrow H_2(v-1) + H_2(v=0)$ V-T process are shown by Capitelli, et al. [21]. This leads to anharmonic vibrational pumping which is well known to be very efficient in $N_2$ and CO molecular plasmas and, in the latter, leads to the population inversion responsible for the CO laser [22-25].

We have constructed a computational model along the lines of that used by Fisher and Kummler [23] that includes electron impact excitation and de-excitation of the vibrational manifold as well as the V-V and V-T processes $H_2$ (v=0) through $H_2$ (v=9) This, admittedly very simple, vibrational excitation model yields the vibrational temperature distributions shown in the next graph for a range of E/N values. The vibrational temperature $T_v$ is defined with respect to $H_2(v=0)$ such that the relative population of $H_2(v)$ is $p(v) = \exp(-\varepsilon_v/T_v)/\Sigma_{v'}p(v')$.

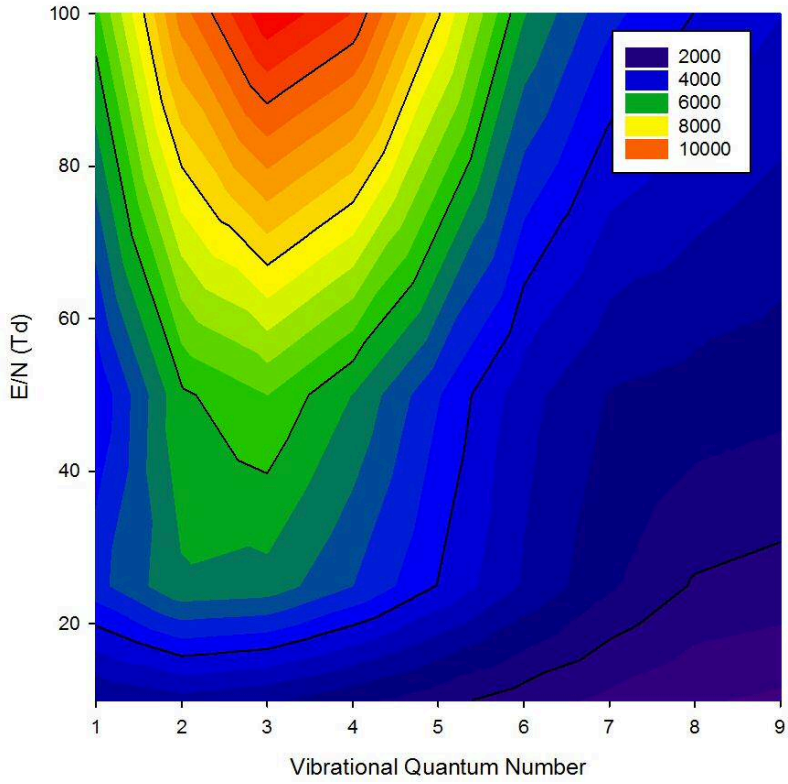


**Figure 5 Computed vibrational temperatures for $H_2$ (v=1) through $H_2$ (v=9).**

The graphs demonstrate that high vibrational temperatures and, consequently, high dissociative attachment rates should be readily attainable in a hydrogen discharge.

Using these calculated vibrational temperatures, we calculated the total attachment and ionization coefficients as functions of E/N. These are graphed in Fig. 6 parametric in the

fractional dissociation δ of $H_2$ where $0 \le \delta \le 1$. The mole fractions of $H_2$ and H are given by $f_{H2} = (1-\delta)/(1+\delta)$ and $f_H = 2\delta(1+\delta)$ respectively.

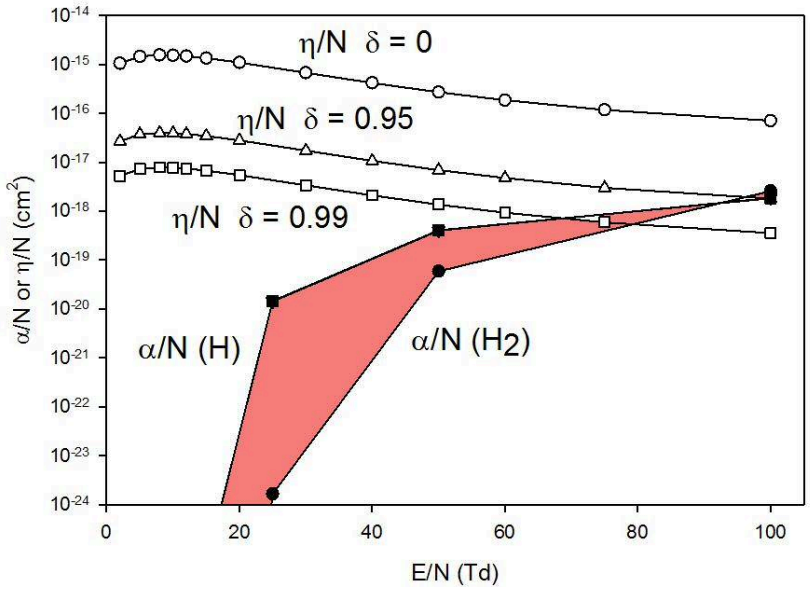


**Figure 6 Ionization coefficients and total dissociative attachment coefficients parametric in fractional dissociation.**

It is clear that at some value of E/N during the changing plasma kinetics the discharge will locally and perhaps transiently be dominated by negative ion formation.

Raizer [26] discusses at length a perturbation approach to understanding instabilities. More specifically Nighan and Wiegand [27] discuss in detail a perturbative analysis, based on the more general theory of Haas [28], of the role that negative ions may play in instabilities associated with volume dominated discharges. An important criterion for instability was shown to be

$$k_a(T_e)\,\kappa_a(T_e)/\,k_i(T_e)\,\kappa_i(T_e) > 1$$

where $k_a$ and $k_i$ are the attachment and ionization rate coefficients. $\kappa(T_e)$ is the logarithmic derivative $\partial\ln(k)/\partial\ln(T_e)$. They were interested in large volume $CO_2$ and CO discharges. In our hydrogen plasma things are more complicated due to the strong vibrational temperature dependence of attachment. We have performed the calculation using the model of the criterion a function of E/N and find that the $H_2$ discharge should be unstable for E/N < 16 Td, which is about the values of the fields in the potential wells of the double layers such as that shown in Fig. 3.

A molecular gas having large dissociative attachment cross sections with small excitation thresholds, such as vibrationally excited $H_2$ (or in the extreme, $F_2$, which has no threshold and a very large cross section at zero energy) has a profound effect upon the distribution of electron energies, i.e. $f_o(\varepsilon)$, in a weakly ionized gas. In Fig. 7 we see $f_o(\varepsilon)$ computed by solving Boltzmann's equation for electrons in $H_2$ in the absence of strong

attachment at vibrational temperatures of 300, 3000, and 5000K. These distributions are as expected with the so-called super-elastic or collisions of the second kind with the excited vibrational states pushing electrons to greater energies.

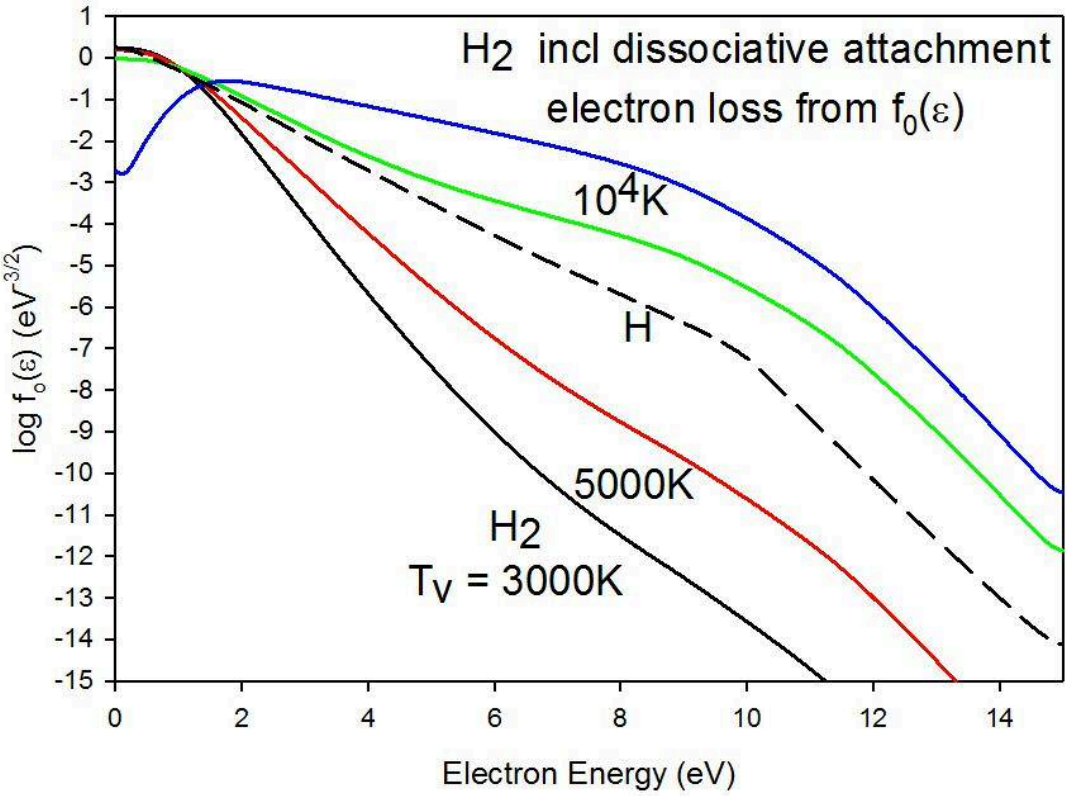


**Figure 7 Computed distributions of electron energies in $H_2$**

On this semi-logarithmic graph a thermal Maxwell-Boltzman distribution where $f_o(\varepsilon) \propto \exp(-\varepsilon/kT_e)$ would be a straight line having a negative slope.

If the gas is strongly attaching electrons are removed from $f_o(\varepsilon)$ rather than simply being moved to lower or higher energies on the energy axis and thus being conserved. Figure 7 also shows such a distribution dominated by dissociative attachment. The normalization of $f_o(\varepsilon)$

$$\int_0^\infty f_o(\varepsilon)\varepsilon^{1/2} d\varepsilon = 1$$

causes the reduced mean energy $2<\varepsilon>/3$, which would $T_e$ for a thermal distribution, to appear quite high. Claiming that there exists an electron temperature $T_e$ associated with such a distribution would be greatly misleading. Note that the same effect on $f_o(\varepsilon)$ may be due to dissociative recombination of $H_2^+$ but would be very small unless the ion density is quite large. In a highly ionized plasma, however, electron-electron collisions

would tend to thermalize the distribution. A large values of E/N low energy secondary electrons from ionization would tend to fill in the electron population at low energies.

The possibility exists that the electron mobility,

$$\mu_e \propto -\int_0^\infty \{[df_o(\varepsilon)/d\varepsilon]/\sigma_m(\varepsilon)\}\varepsilon d\varepsilon$$

could be negative in a strongly attaching gas due to $df_o(\varepsilon)/d\varepsilon > 0$ at low energies. This would cause electrons to drift with the E-field vector rather than against it. This situation would, presumably, lead to instability. Dyatko, et al. [29] have calculated the same phenomenon in a model problem involving a mixture of Ar and $F_2$ finding, indeed, a drift velocity that rises positively from near zero at very small E/N and then, at some point falls through zero to a negative value before rising again through zero and increasing positively again. Although not a result of electronegativity this phenomenon has been measured in Xe at very small values of E/N [30].

We have performed time dependent kinetics of the plasma chemistry described above in zero spatial dimensions using the E/N dependent rate coefficients and vibration temperatures. An example calculation is shown in Figure 8. As we would expect at large E/N the fractional dissociation of $H_2$ is close to unity but as E/N decreases the $H^-$ negative ion density increases while the electron density decreases. Ultimately the controlling processes are $H + H^- \rightarrow H_2 + e$ and $H_2^+ + H^- \rightarrow H_2 + H$.

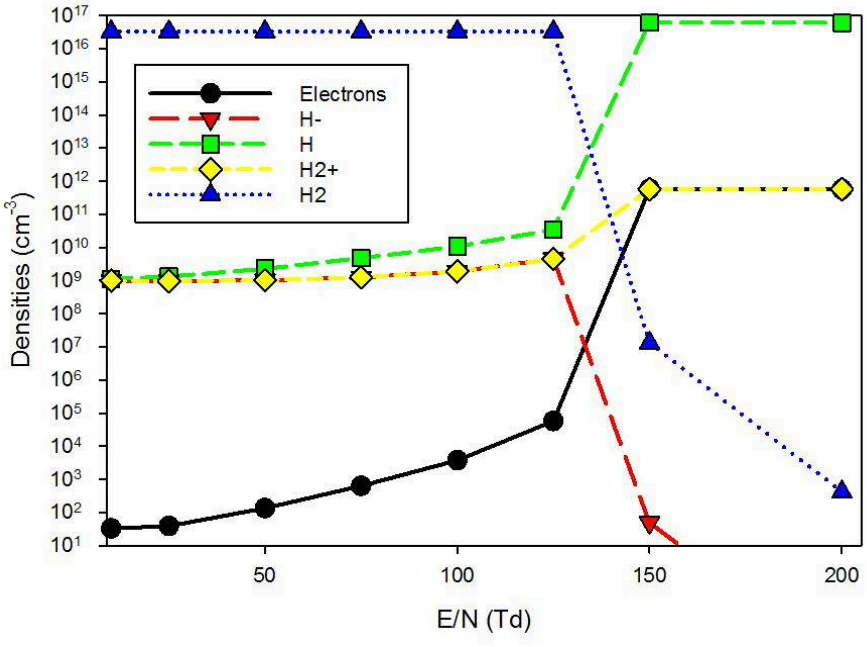


**Figure 8 Calculated steady state densities of species as functions of E/N. The density was $3.3 \times 10^{16} cm^{-3}$ and the gas temperature was 1000 K.**

Performing the calculations discussed above indicates that, in $H_2$ at values of E/N < 25 Td or so as are found in the vicinity of the striations, the propensity to instability exists. One could, in principle, perform completely self-consistent calculations including all collisional processes, V-V and V-T processes, dissociative attachment to vibrationally excited states of $H_2$, electron and ion drift and diffusion, and the solution of Poisson's equation $\nabla \bullet E + 4\pi e(N_+ - N_e - N_-)$ including self-consistent positive ion ($N_+$), electron ($N_e$), and negative ion ($N_-$) densities. Boeuf, et al. [31] have performed such calculations in time and one-dimension for a linear discharge in $CF_4$. Peres and Pitchford [32] have performed similar calculations for a model electronegative gas mixture in a DC glow discharge. Sukhinin and Fedoseev [33] modeled moving striations in Ar using the drift-diffusion fluid formulation in the spherical geometry but found that their numerical scheme was unstable when they tried to find steady solutions. In addition they did not consider an electronegative gas.

Nerushev, et al. [2] and Belikov and Sakhapov [7] have tried to relate the existence of the striations to the possibility of having a negative differential conductivity in the gas mixture. In most gases the electron drift velocity $V_d(E/N)$ is a strictly monotonically increasing function of E/N. Famously, in the rare gases Ar, Kr, and Xe, which have Ramsauer minima in their electron collision momentum transfer cross sections, the slope of $V_d[E/N]$ can be negative over a certain range of values of E/N. Since the electrical conductivity $\sigma \propto V_d(E/N)$ its differential can become negative. Hence the term negative differential conductivity. This topic was explored extensively by Petrovic, et al. [34]. Belikov and Sakhapov present calculations for an $N_2$-acetone mixture showing a region of $dV_d(E/N)/d(E/N) < 0$ over a range $\sim 0.5\ T_d < E/N < \sim 1.5\ T_d$. Neither they nor Nerushev, et al. present a model showing how this phenomenon leads to striations. In calculations using model cross sections, however, Vrhovac and Petrovic [35] have shown how attachment can lead to negative differential conductivity. It becomes increasingly clear that attachment and negative ion formation play a major role in the formation of the double layers and striations that we have been discussing here.

### C. Perturbations leading to instability

There are a number of processes that could perturb the plasma leading to the striations. In none of the experiments does the geometry have perfect spherical symmetry. Other features of ours and the Russian experiments are the very steep electric potential and field gradients due to the small size of the high voltage anode. We observed that our iron anode was very hot, which would lead to a strong temperature gradient in the gas.

As early as 1941 Cobine [36] commented on the complexity of anode sheaths in electronegative gases and their dependence upon anode size. Models of sheaths in electronegative gases are discussed in some detail by Lieberman and Lichtenberg [37] but the controversy concerning such models can be seen in the critique by Franklin [38]. We suspect that the anode sheaths and potential drop in a gas dominated by negative ions in this high aspect ratio spherical geometry are easily perturbed and that the perturbations

near the anode cause changed in the space charge radially outward from the anode. Perhaps a much larger anode would exhibit greater stability.

If in the spherical geometry the anode had radius $R_a$ and the cathode or ground is a sphere of radius $R_c$ then the steady state temperature distribution [39] along $R_a \le r \le R_c$ is

$$T(r) = [R_a T_a(R_c - r) + R_c T_c(r - R_a)]/r(R_c - R_a)$$

If $R_c >> R_a$ then the temperature in the vicinity of the anode is

$$T(r)/T_a \simeq R_a/r + T_c(1 - R_a/r)/T_a$$

So, the gas temperature declines rather slowly with distance from the anode surface.

That our anode was hot can be seen from the following photo.

**Figure 9 ¼" (~0.6 cm) diameter iron anode after use in a hydrogen discharge.**

Anode temperature fluctuations can be propagated into the gas having the effect of changing the gas density and hence E/N and the space charge density.

Our iron anode, unlike those made of copper tungsten, has a unique specific heat temperature dependence $C_v(T)$ that peaks sharply at the Curie temperature of 1043 K. It increases from a value of 43 J/mol/K at 900 K to 84 J/mol/K at 1043 K, and back down to 43 J/mol/K at 1100 K. Since the heating rate of the anode of volume V is

$$dT/dt = P/\rho C_v V$$

the rate of temperature change with power P will fluctuate by a factor of two over a very small temperature increment. This could cause thermal waves to propagate out from the anode.

## V. CONCLUSION

In our initial small scale experiments using a small iron electrode in a glass bell jar we have found that we obtain the spherically striated, i.e. concentric shells, hydrogen discharge in the pressure range 0.7 Torr < p < 3 Torr. We have had such discharges that were stable for several minutes. Others such as that shown in Fig. 10 below, operating at about 0.8 Torr, switched modes every 3-4 seconds.

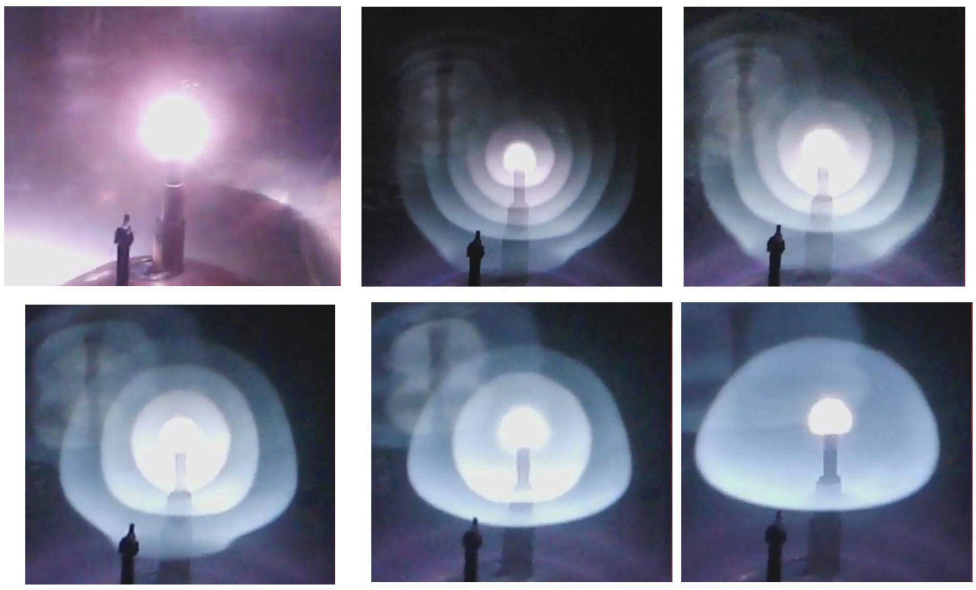

**Figure 10 Sequence of frames from a video of striation formation in a hydrogen. The lighter shifted images are reflections from the wall of the bell jar vacuum chamber.**

This may have something to do with anode temperature fluctuations near the Curie temperature of the iron anode.

That all the publications that we have seen on striated spherical plasmas have used gases that dissociate and dissociatively attach electrons is telling. We have proposed that negative ions may be responsible for the observed double layer instability in all these experiments. Ours is the only such experiment that we know of that has been performed in hydrogen. As we have stated above we think that in $H_2$ the processes of vibrationally enhanced dissociative attachment of $H_2(v)$, electron impact dissociation of $H_2$ in H atoms, and the balancing effect of associative detachment $H^- + H \rightarrow H_2 + e$ conspire to drive the observed instabilities.

Our future experiments will take place in a larger vacuum chamber, allow the use of a larger anode, have a DC power supply having higher voltage and current capability, and, importantly, make use of Langmuir probes in order to study these phenomena.

## ACKNOWLEDGEMENTS

We are pleased to thank J. Onderco for technical assistance, M. Clarage and P. Anderson for their contributions to this research, and the International Science Foundation for financial support. WLM would like to dedicate the article to the late Dr. A. V. Phelps and the late Prof. E. R. Fisher, mentors and friends for four decades from whom he learned much of the physics upon which this research has been based.

## References


1. O. A. Nerushev, S. A. Novopashin, V. V. Radchenko, and G. I. Sukhinin, JETP Lett. **66**, 711 (1997).
2. O. A. Nerushev, S. A. Novopashin, V. V. Radchenko, and G. I. Sukhinin, Phys. Rev. E **58**, 4897 (1998).
3. S. A. Novopashin, A. A. Polyakov, V. V. Radchenko, and S. Z. Sakhapov, Tech. Phys. Letts **33**, 196 (2007).
4. S. A. Novopashin, V. V. Radchenko, and S. Z. Sakhaporov, J. Engr. Thermophys. **17**, 71 (2008).
5. S. A. Novopashin, V. V. Radchenko, and S. Z. Sakhapov, IEEE Trans Plas. Sci. **36**, 998 (2008).
6. A. V. Fedoseev and G. I. Sukhinin, J. Engr. Thermophys. **17**, 74 (2008).
7. A. E. Belikov and S. Z. Sakhapov, J. Phys. D **44**, 045202 (2011).
8. R. S. Sigmond, J. Appl. Phys. **53**, 891 (1982).
9. J. L. Pack and A. V. Phelps, Phys. Rev. **121**, 798 (1961).
10. A. V. Phelps, Plas. Sources Sci. Technol. **20**, 043001 (2011).
11. M. Capitelli, R. Celiberto, F. Esposito, A. Laricchiuta, K. Hassouni, and S. Longo, Plas. Sources. Sci. Technol. **11**, A7 (2002).
12. M. Capitelli, R. Celiberto, G. Colonna, G. D'Ammondo, O. DePasCale, P. Diomede, F. Esposito, C. Gorse, A. Laricchiuta, S. Longo,and L. D. Pietanza, J. Phys. B **43**, 144025 (2010).
13. M. Capitelli, O. DePascale, P. Diomede, A. Gicquel, C. Gorse, K. Hassouni, S. Longo, and D. Pagano, AIP Conf. Proc. **763**, 66 (2005).
14. S. J. Buckman and A. V. Phelps, J. Chem. Phys. **82**, 4999 (1988).
15. R. Celiberto, R. K. Janev, A. Laricchiuta, M. Capitelli, J. M. Wadehra, and D. E. Atems, At. Data and Nucl. Data Tables **77**, 161 (2001).
16. S. Pancheshnyi, S. Biagi, M. C. Bordage, G.J.M. Hagelaar, W. L. Morgan, A. V. Phelps, and L. C. Pitchford, Chem. Phys. **398**, 148 (2012).
17. W. L. Morgan and B. M. Penetrante, Comp Phys Comm. **58**, 127 (1990).
18. A. I. Floresu – Mitchell and J.B.A. Mitchell, Physics Reports **430**, 277 (2006).
19. D. McElroy, C. Walsh, A. J. Markwick, M. A. Cordiner, K. Smith, and T. J. Millar, Astron. Astrophys. **550**, A36 (2013); The UMIST Database for Astrochemistry, udfa.ajmarkwick.net
20. J. C. Y. Chen, J. Chem. Phys. **40**, 3513 (1964).
21. M. Capitelli, R. Celiberto, and M. Cacciatore, in *Advances in Atomic and Molecular Physics* **33**, ed. M. Inohuti (Academic Press, San Diego, 1994).
22. R. C. Millikan and D. R. White, J. Chem. Phys. **39**, 3209 (1963).
23. E. R. Fisher and R. H. Kummler, J. Chem. Phys. **49**, 1095 (1968).
24. G. E. Caledonia and R. E. Center, J. Chem. Phys. **55**, 552 (1971).
25. J. D. Lambert, *Vibrational and Rotational Relaxation in Gases* (Clarendon, Oxford, 1977).
26. Y. P. Raizer, *Gas Discharge Physics* (Springer-Verlag, Berlin, 1991).
27. W. L. Nighan and W. J. Wiegand, Phys. Rev. A **10**, 922 (1974).
28. R. A. Haas, Phys. Rev. A **8**, 1017 (1973).

29. N. A. Dyatko, A. P. Napartovich, S. Sakadzic, Z. Petrovic, and Z. Raspopovic, J. Phys. D **33**, 375 (2000).
30. J. M. Warman, U. Sowada, and M. P. DeHaas, Phys. Rev. A **31**, 1974 (1985).
31. J. P. Boeuf, L. C. Pitchford, and W. L. Morgan, *22nd Int. Conf. On Phenom. Ioniz. Gases (ICPIG),* Hoboken (1995).
32. I. Peres and L. C. Pitchford, J. Appl. Phys. **78**, 774 (1995).
33. G. I. Sukhinin and A. V. Fedoseev, *Int. Conf. On Ionized Gases (ICPIG) Proceedings* **4**, 143 (2003).
34. Z. Lj. Petrovic, R. W. Crompton, G. N. Haddad, Aust. J. Phys. **37**, 23 (1984).
35. S. B. Vrhovac and Z. Lj. Petrovic, Phys. Rev. E **53**, 4012 (1996).
36. J. D. Cobine, *Gaseous Conductors*, (Dover, NY, 1958).
37. M.A. Lieberman and A. J. Lichterberg, *Principles of Plasma Discharges and Materials Processing* (Wiley, NY, 1994).
38. R. N. Franklin, Plas. Sources Sci. Technol. **10**, 162 (2001).
39. H. S. Carslaw and J. C. Jaeger, *Conduction of Heat in Solids* (Clarendon Press, Oxford, 1959).